JGR Oceans

Key Points:

- Measurements from three buoys used to validate surface meteorology in the ERA-Interim and ERA5 reanalyses over the Weddell Sea
- Both reanalyses represent variability well but have a warm bias in surface air temperature
- Warm bias may result from the simplified representation of sea ice in the reanalysis models

Correspondence to:
J. C. King,
jcki@bas.ac.uk

The Performance of the ERA-Interim and ERA5 Atmospheric Reanalyses Over Weddell Sea Pack Ice

John C. King[1] , Gareth J. Marshall[1] , Steve Colwell[1] , Stefanie Arndt[2] , Clare Allen-Sader[1] , and Tony Phillips[1]

[1]British Antarctic Survey, Cambridge, UK, [2]Helmholtz Centre for Polar and Marine Research, Alfred Wegener Institute, Bremerhaven, Germany

Abstract We use meteorological measurements from three drifting buoys to evaluate the performance of the ERA-Interim and ERA5 atmospheric reanalyses from the European Center for Medium-Range Weather Forecasts over the Weddell Sea ice zone. The temporal variability in surface pressure and near-surface air temperature is captured well by the two reanalyses but both reanalyses exhibit a warm bias relative to the buoy measurements. This bias is small at temperatures close to 0°C but reaches 5–10°C at −40°C. For two of the buoys the mean temperature bias in ERA5 is significantly smaller than that in ERA-Interim while for the third buoy the biases in the two products are comparable. 10 m wind speed biases in both reanalyses are small and may largely result from measurement errors associated with icing of the buoy anemometers. The biases in downwelling shortwave and longwave radiation are significant in both reanalyses but we caution that the pattern of bias is consistent with potential errors in the buoy measurements, caused by accumulation of snow and ice on the radiometers. Overall, our study suggests that, with the exception of near-surface temperature, both reanalyses reproduce the buoy measurements to within the limits of measurement uncertainty. We suggest that the significant biases in near-surface air temperature may result from the simplified representation of sea ice used in the reanalysis models, and we recommend the use of a more sophisticated representation of sea ice, including variable ice and snow thicknesses, in future reanalyses.

Plain Language Summary The Antarctic sea ice zone plays a central role in driving the global ocean circulation and in controlling global climate. Much of our understanding of Antarctic sea ice and its variability comes from using coupled ice-ocean models, which are forced using atmospheric data. Global atmospheric "reanalyses" (gridded fields of atmospheric data produced using the same models that are employed in numerical weather prediction) are often used for this purpose, but little is known about the reliability of these products in the polar regions. We have used meteorological measurements from three drifting buoys that were deployed in the Weddell Sea (Antarctic) to evaluate the performance of two reanalysis products. We found that both reanalyses had a good representation of day-to-day variations in meteorological conditions (pressure, temperature, humidity, wind, and radiation). However, temperatures in both reanalyses were biased warm, with the largest biases seen during the coldest part of the Antarctic winter. The biases probably result from the use of a very simple representation of sea ice in the reanalysis models. We recommend that a more sophisticated representation should be used in future reanalyses.

1. Introduction

The Weddell Sea is an important component of both the Antarctic and global climate systems. It is one of the largest sources of Antarctic bottom water (AABW), which is a major component of the Atlantic Ocean meridional overturning circulation. Sea ice plays a major role in the creation of the dense water masses that are precursors to AABW. It is, therefore, important to have a detailed understanding of the processes that control the formation, decay, and movement of sea ice in this region.

In the absence of long-term direct observations, ice-ocean models (Neme et al., 2021; Timmermann et al., 2002) have provided us with important insight into these processes. Unlike fully coupled climate models, ice-ocean models are driven by specifying surface values of atmospheric forcing variables, including wind (or surface stress), air temperature, humidity, precipitation and radiation, which can be conveniently obtained from the gridded atmospheric reanalyses produced by a number of centers, including the European Center for Medium-Range Weather Forecasts (ECMWF). Ice-ocean model results have been shown to be sensitive to the details of surface

Validation: Steve Colwell, Clare Allen-Sader
Visualization: John C. King, Tony Phillips
Writing – original draft: John C. King
Writing – review & editing: Gareth J. Marshall, Steve Colwell, Stefanie Arndt, Clare Allen-Sader, Tony Phillips

forcing (Stössel et al., 2011) so, before using these products to force models, it is important to determine how well the reanalysis represents the forcing variables across the area of interest, which requires independent observational data for validation of the reanalysis. As the sea ice covered regions of the Southern Ocean are difficult to access, particularly during winter, there is a lack of suitable validation data and only a limited number of validation studies have been carried out. King (2003) validated ECMWF operational surface pressure analyses over the Bellingshausen Sea using data from two drifting buoys that were operational during February–May 2001 and found a root mean square (RMS) difference between analysis and observed pressures of around 1 hPa. This very small difference indicates that the analysis is capable of reproducing the observed pressure field with high accuracy in a region that is almost devoid of in situ observations, which suggests that the analysis is well-constrained by remote sensing measurements, particularly from temperature sounders. The performance of operational analyses from ECMWF and reanalyses produced by the National Centers for Environmental Prediction (NCEP)/National Center for Atmospheric Research (NCAR) over the central Weddell Sea was studied by Vihma et al. (2002) using data from two meteorological buoys that drifted northwards in the pack ice between February 1996 and January 1997. They found a mean warm bias of 3.5°C in air temperatures from the ECMWF product while the NCEP/NCAR reanalysis had a corresponding cold bias of 3.2°C, with the largest biases seen at the lowest temperatures in both products. Jonassen et al. (2019) used observations made at the drifting camp Ice Station Weddell during 1992 to validate the ECMWF ERA-Interim reanalysis and found a mean warm bias in air temperature of around 2.5°C, with the largest biases again found at the lowest temperatures. Biases in downwelling shortwave and longwave radiation in the reanalysis were found to be insignificant.

In this study, we use measurements from three meteorological buoys that drifted through the Weddell Sea pack ice between January 2016 and February 2017 to validate the performance of the latest ECMWF reanalysis, ERA5, in this region for the first time. We also validate the older ERA-Interim reanalysis for comparison. The buoys were equipped with sensors to measure pressure, air temperature, humidity, wind speed and direction and radiation, which has enabled us to validate the surface variables in the reanalyses comprehensively. The buoy measurements and reanalyses are described in Section 2 below. In Section 3, we present the results of our validation study and, in Section 4, we discuss the strengths and weaknesses of the reanalyses as forcing data for ice-ocean models.

2. Data and Methods

2.1. Drifting Buoy Measurements

We make use of meteorological data collected from three drifting buoys, designated 2016A3, 2016A4, and 2016A5, henceforth referred to as A3, A4, and A5 for brevity, that were deployed by the Alfred Wegener Institute from R/V *Polarstern* in the southeastern Weddell Sea during January 2016. The buoys were constructed by the British Antarctic Survey and were equipped with the meteorological sensors listed in Table 1. Wind speed and direction (relative to the buoy orientation) were measured using a propeller-vane wind monitor (R M Young model 05106) mounted approximately 2 m above surface level. A magnetic compass (PNI TCM2.5) provided a measurement of buoy orientation that was used to transform the relative wind direction measurement from the wind monitor

Table 1
Details of the Meteorological Sensors Carried by the Buoys

Variable	Sensor	Accuracy
Pressure	Vaisala PTB 110	±1 hPa
Air temperature	Campbell Scientific CS215	±0.4°C
Relative humidity	Campbell Scientific CS215	±2%
Wind speed	Young 05103 Wind Monitor	±0.3 m s⁻¹
Wind direction	Young 05103 Wind Monitor + PNI TCM2.5 compass	±5°
Downwelling shortwave radiation	Campbell Scientific CS300	±5%
Downwelling longwave radiation	Hukseflux IR02	±10%

Note. Quoted accuracies are manufacturers' figures for the sensor under ideal conditions and do not take into account errors due to icing or other environmental factors.

into an absolute direction. Air temperature and relative humidity were measured using a Campbell Scientific CS215 sensor mounted in a miniature naturally ventilated radiation shield at approximately 1.5 m. The buoys also carried a second temperature sensor (Campbell Scientific PT100/3) but data from this sensor were not used in this study due to concerns regarding its calibration. Downwelling short- and longwave radiation were measured using a Campbell Scientific CS 300 Apogee pyranometer and a Hukseflux IR02 pyrgeometer, respectively. Atmospheric pressure was measured using a Vaisala PTB 110 sensor. All sensors were individually calibrated by their manufacturers. The buoy locations were obtained using an onboard Global Positioning System (GPS) receiver and hourly measurements from all sensors were transmitted via the Iridium satellite communications system. Further information on the buoys can be found at https://data.seaiceportal.de/gallery/index_new.php?active-tab1=method%26buoytype=AB%26region=s%26buoystate=all%26expedition=all%26buoynode=all%-26submit3=display%26lang=en_US%26active-tab2=buoy.

All sensors generally performed well but manual inspection of the data revealed a few issues. There were some periods when no GPS location fixes were available, probably due to snow accumulating on the GPS antenna. For buoys A3 and A4 these periods generally last no longer than 1–2 days but, for buoy A5, location data became unreliable from 3 November 2016 until the loss of transmissions from the buoy on 22 December 2017 and we have not used data from A5 during this period in our analysis. There are also a number of occasions when the wind speed was recorded as zero over several hours, almost certainly indicating icing of the wind monitor propeller. These periods, totaling around 5 days of data for A3, 11 days for A4, and 5 days for A5 were removed from the wind data and also from the radiation data since icing will affect the performance of the radiometers. It is possible that sensors were being affected to a lesser extent by ice and/or snow accumulation on other occasions but there is no way to verify this, and we assume that the quality control checks described here have excluded the worst-affected data. Around 90% of the icing events detected occurred during the colder months of April through September.

Relative wind directions were converted to absolute magnetic directions using the buoy compass and were then corrected to true directions using the International Geomagnetic Reference Field (www.ngdc.noaa.gov/IAGA/vmod/igrf.html). The compass on buoy A3 failed on deployment so no wind directions are available from this buoy. A preliminary comparison of buoy wind directions with those from the ECMWF reanalyses suggested that there was a systematic wind direction error from buoys A4 and A5, which could have resulted from misalignment of the wind monitor relative to the compass. In order to compensate for this an offset of 15° has been subtracted from the wind directions measured by both of these buoys. Relative humidity measurements were corrected using the procedure described by Anderson (1994).

The locations of the buoy deployments are given in Table 2 and the drift of the buoys subsequent to deployment is shown in Figure 1. Buoys A3 and A5 were both deployed on large ice floes within the drifting pack ice. Both buoys drifted northwards through the winter of 2016 and entered the retreating marginal ice zone during the austral spring of that year. Buoy A4 was deployed in near-coastal fast ice. After about two weeks, the fast ice broke out and the buoy drifted westwards until 1 February when it once again became trapped in coastal fast ice just off the Stancomb Wills Glacier Tongue (around 73.9°S, 23.7°W), where it remained through the winter of 2016 before drifting westwards from mid-January 2017.

Table 2
Details of the Buoy Deployments

Buoy	Deployment date	Deployment location	Ice type	Ice thickness (m)	Snow thickness (m)	End date	End location
A3	15 January 2016	76.54°S 47.04°W	Multi-year ice	2.32	0.25	28 February 2017	65.25°S 51.56°W
A4	27 January 2016	72.80°S 19.34°W	Fast ice	3.30	0.32	1 February 2017	74.37°S 28.07°W
A5	25 January 2016	75.47°S 31.41°W	First-year ice	1.44	0.39	2 November 2016	65.15°S 31.84°W

Note. Snow and ice thickness and ice type are as recorded at the deployment location.
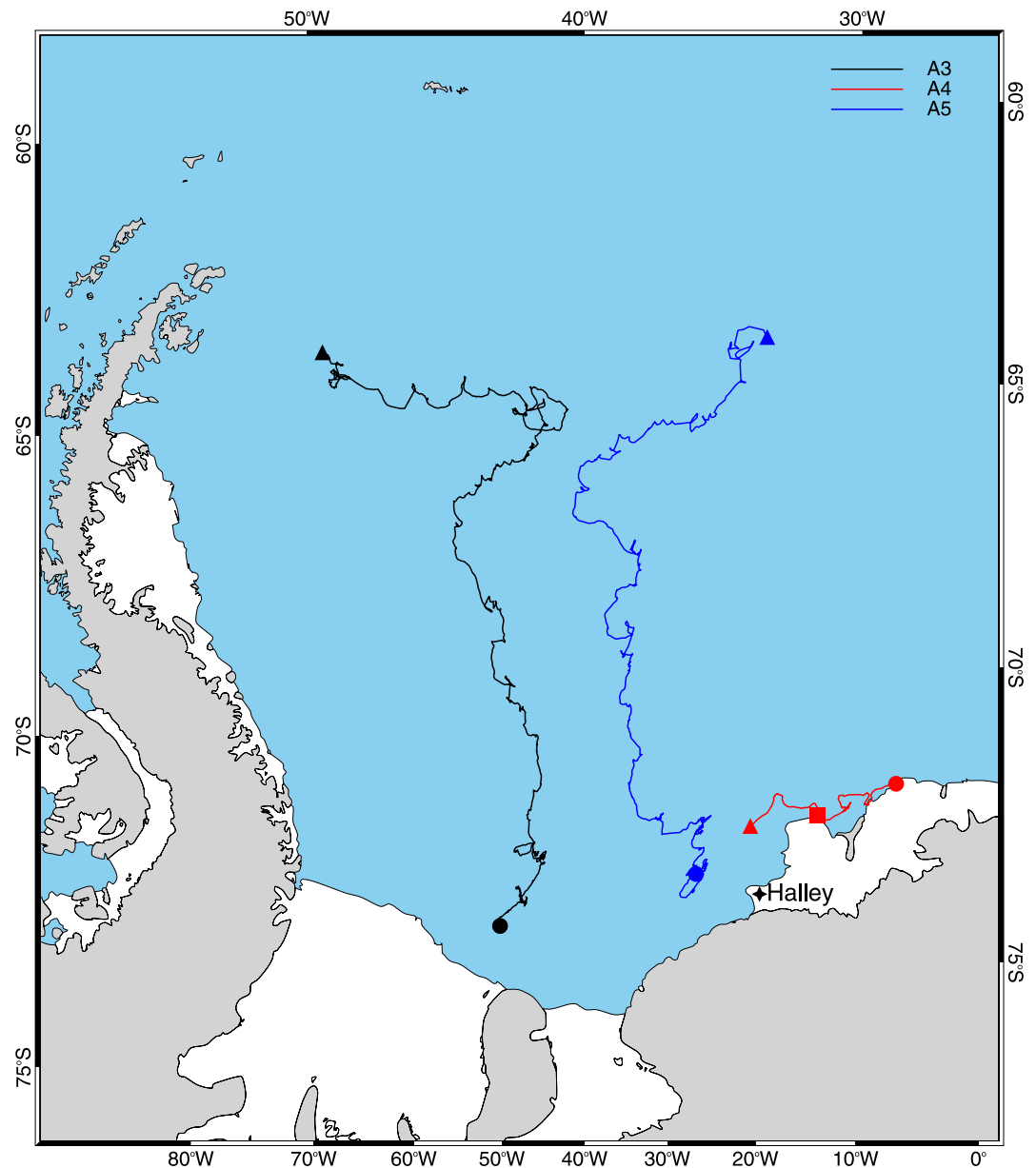
Figure 1. Drift tracks of the three buoys: A3 (black), A4 (red), and A5 (blue). Filled circles indicate the buoy deployment positions, filled triangles indicate the end of the drift track (see Table 1 for dates). The filled red square indicates the location where A4 was stationary in coastal fast ice between February 2016 and January 2017 and the position of Halley Research Station is marked. Ocean is shaded in light blue, ice shelves in white and land/grounded ice in gray.

Buoy A3 was deployed together with a Snow Buoy (Nicolaus et al., 2021, identifier 2016S38) and an Ice Mass Balance buoy (IMB, Jackson et al., 2013, identifier 2016T37). Buoy A4 was deployed with an IMB (identifier 2016T40) and A5 with a Snow Buoy (2016S40) and an IMB (2016T38). These autonomous systems provide additional information on the sea ice thickness and snow depth evolution, as well as air temperature and (Snow Buoys only) pressure. Observations from A3, A4, and A5 were not made available to the Global Telecommunications System (GTS) of the World Meteorological Organization and hence potentially provide an independent source of data for validating atmospheric reanalyses. However, pressure measurements from the Snow Buoys were transmitted on the GTS and were assimilated by the ERA5 reanalysis for at least part of the study period (S. Keeley, ECMWF, pers. comm., 14 July 2022) so pressure measurements from the adjacent meteorological buoys (A3 and A5) are not strictly independent of the reanalyses.
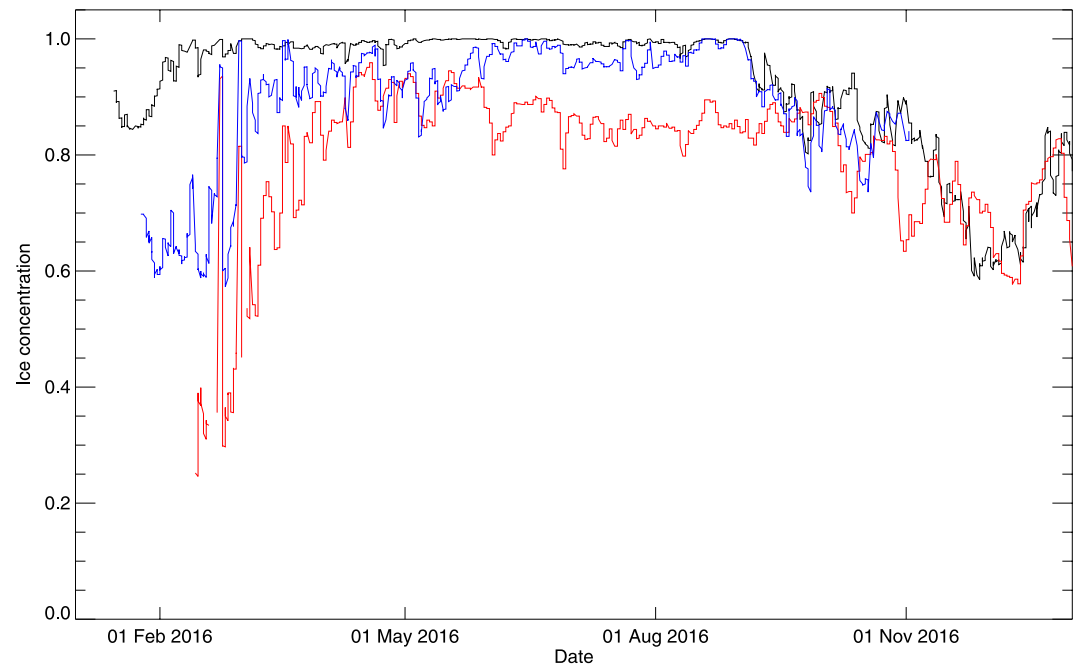
Figure 2. Sea ice concentration along the drift tracks of buoy A3 (black), buoy A4 (red), and buoy A5 (blue) interpolated from the ERA-Interim ice concentration field. Ice concentrations from ERA5 are similar.

Figure 2 shows the sea ice concentration at the locations of all three buoys interpolated from the ice concentration fields used in the ERA-Interim reanalysis (see Section 2.2 for details). Ice concentration at the locations of buoys A3 and A5 remained high (generally greater than 0.9) throughout the winter of 2016. At the location of A4, the ice concentration was consistently lower—typically between 0.8 and 0.9 during the winter. As this buoy remained in fast ice through the 2016 winter we can assume that the *local* ice concentration was actually close to 1 throughout this period. However, the ERA-Interim ice product reflects ice concentration on the model grid scale (around 80 km for ERA-Interim). On this spatial scale, the presence of persistent coastal polynyas along this part of the Antarctic coast (Markus et al., 1998) will reduce the mean ice concentration in the ERA-Interim grid cell surrounding buoy A4.

2.2. ECMWF Atmospheric Reanalyses

We have used the buoy measurements to validate two atmospheric reanalyses produced by the ECMWF. The ERA-Interim reanalysis (Dee et al., 2011) was first released in 2006 and is based on cycle 31r2 of the ECMWF Integrated Forecast System (IFS) model. This model has a horizontal resolution of around 80 km and has 60 vertical levels between the surface and the model top at 0.1 hPa. Output data are available at six-hourly intervals. In 2019, ERA-Interim was superseded by the ERA5 reanalysis (Hersbach et al., 2020). ERA5 is based on cycle 41r2 of the IFS model, which has a higher horizontal resolution (around 30 km), more vertical levels (137) and a higher model top (0.01 hPa) as well as updated model physics. ERA5 output data are provided at hourly intervals.

While the atmospheric model used in ERA5 is a significant improvement over that used for ERA-Interim, both reanalyses use similar simple representations of sea ice to provide a lower boundary condition. In both reanalyses sea surface temperatures are obtained from the OSTIA (Operational Sea-surface Temperature and sea Ice Analysis) product (Donlon

Table 3
Validation Statistics for Reanalysis Mean Sea Level Pressure Interpolated to Buoy Locations (Units: hPa)

Buoy	Reanalysis	ERA mean	Buoy mean	Bias	RMSE	r
A3	ERA-Int.	986.76	986.83	−0.07	0.50	0.999
A3	ERA5	986.91	986.80	0.11	0.47	0.999
A4	ERA-Int.	984.27	984.48	−0.21	0.64	0.992
A4	ERA5	984.77	984.48	0.29	0.61	0.999
A5	ERA-Int.	983.95	983.86	0.08	0.60	0.999
A5	ERA5	984.22	983.86	0.36	0.61	0.999

Note. Bias is reanalysis minus buoy observation.

Table 4
Validation Statistics for Reanalysis Air Temperature Interpolated to Buoy Locations (Units: °C)

Buoy	Reanalysis	ERA mean	Buoy mean	Bias	RMSE	r
A3	ERA-Int.	−11.48	−12.62	1.14*	2.40	0.977
A3	ERA5	−12.41	−12.62	0.22	2.66	0.978
A4	ERA-Int.	−12.64	−14.82	2.18*	4.37	0.951
A4	ERA5	−12.09	−14.82	2.73*	4.69	0.960
A5	ERA-Int.	−14.73	−15.31	0.59	2.57	0.953
A5	ERA5	−15.20	−15.31	0.11	2.44	0.956

Note. Columns are as for Table 3. An asterisk indicates that the bias is statistically significant at the 5% level or better.

et al., 2012), which is also used to specify sea ice concentrations (SICs) in ERA-Interim. SICs in ERA5 are obtained from the OSI SAF product (Lavergne et al., 2019). Where sea ice is present within a grid box, an ice surface temperature is calculated using a fixed ice thickness of 1.5 m with no snow layer on top of the sea ice layer. Surface fluxes are computed separately for the ice-covered and open water fractions of a grid box and are then combined as a weighted average.

2.3. Comparison of Buoy and Reanalysis Data

Although ERA5 provides data at 1-hr intervals we have chosen to compare both reanalyses with 6-hr data (00, 06, 12, and 18 UTC) for consistency. Reanalysis data were bilinearly interpolated to buoy locations at these times using data from surrounding gridpoints. Sea ice concentration at these points may differ from that at the buoy location but, as ice concentrations remained high at A3 and A5 during most of their drift (Figure 2), errors due to the use of a simple interpolation scheme should be small. For buoy A4, which remained close to the coast, the interpolation may have at times made use of data from land grid points, which may not be representative of the buoy environment. Outputs from the reanalyses include air temperature at 2 m, which can be directly compared with buoy measurements at approximately 1.5 m, and water vapor mixing ratio (ERA-Interim) or dew point (ERA5) at 2 m which we compare with the mixing ratio computed from the buoy relative humidity measurements. Before comparison with 10 m wind data from the reanalyses, buoy wind speeds, measured at approximately 2 m, were extrapolated to 10 m height assuming a logarithmic profile with a roughness length of 5 mm, which is typical of high-concentration snow-covered ice in the Weddell Sea (Andreas et al., 2005; Wamser & Martinson, 1993; Weiss et al., 2011). This correction procedure assumes that the atmospheric boundary layer is neutrally stratified, which may lead to errors, particularly at low wind speeds. However, for a 2 m wind speed of 5 m s^{-1} and a downward (stable) heat flux of 40 W m^{-2}, typical of conditions encountered in the study region, the error due to omitting the stability correction term is less than 10%. This is smaller than the ~20% uncertainty associated with the roughness length varying over a plausible range of 0.05–0.001 m. For the radiation components, we compare the daily mean of hourly buoy measurements with a reanalysis mean computed from the daily sum of reanalysis radiation at the mean position of the buoy during the day.

We calculate the reanalysis mean bias, root mean square error (RMSE), and Pearson correlation coefficient, r, for each variable. The statistical significance of the mean biases is assessed using a *t*-test. Most statistics are presented for the full period of operation of each buoy but, for air temperature, we have also calculated biases for November–February ("extended summer") and April–August ("extended winter"). These season definitions were chosen as they represent periods of relatively stable temperatures and ice concentrations at the locations of buoys A3 and A5.

3. Results

3.1. Pressure

Table 3 shows validation statistics for mean sea level pressure (mslp) at the buoy locations in both reanalyses. Pressures in both reanalyses closely match the buoy measurements, with both mean biases and RMSEs lying well within the quoted sensor accuracy of ±1 hPa. Correlation coefficients exceed 0.99 for all buoy/reanalysis combinations indicating that both reanalyses capture the spatial and temporal variation of mslp over the region with a high degree of accuracy. As noted above, the availability of pressure measurements from
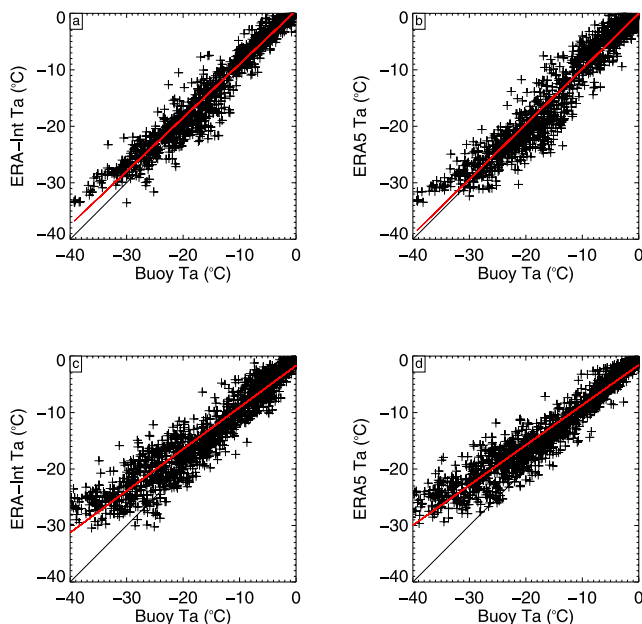

Figure 3. Six-hourly values of reanalysis near-surface air temperature, Ta, plotted against measurements from buoy A3 (panels (a) and (b)) and buoy A4 (panels (c) and (d)). The red lines are least squares regression fits to the data and the black lines indicate perfect agreement.

Table 5

Mean Biases for Air Temperature Interpolated to Buoy Locations (Units: °C) for the Extended Summer (November–February) and Extended Winter (April–August) Seasons

Buoy	Reanalysis	Mean bias		
		All data	November —February	April—August
A3	ERA-Int.	1.14	1.20	1.20
A3	ERA5	0.22	0.88	−0.32
A4	ERA-Int.	2.18	0.39	3.54
A4	ERA5	2.73	0.50	4.34
A5	ERA-Int.	0.59	0.65	0.54
A5	ERA5	0.11	0.80	−0.10

Snow Buoys adjacent to A3 and A5 may have inflated the performance metrics for these locations. However, the metrics for A4, which provided a truly independent pressure measurement, are similar to those for A3 and A5. The high performance of the reanalyses found here is in line with previous studies of the accuracy of pressure fields in ECMWF products at high southern latitudes (King, 2003) and suggests that these products should be able to provide a good description of the surface wind field and its variability on synoptic to seasonal timescales.

3.2. Temperature and Humidity

Validation statistics for air temperature are shown in Table 4. Both reanalyses are biased warm relative to all three buoys, with the ERA-Interim biases all exceeding the quoted sensor accuracy of ±0.4°C. For the two buoys that drifted through the central Weddell Sea (A3 and A5), the ERA5 biases are much smaller than those for ERA-Interim and are not statistically significant. Correlation coefficients for temperature are lower than those for mslp but still exceed 0.95 for all buoy/reanalysis combinations. Scatter plots of reanalysis temperatures against buoy temperatures (Figure 3) show that the warm bias in the reanalyses generally increases with decreasing temperatures and, for all buoys, the largest biases are seen at the lowest temperatures ($T_a < −30°C$). There is little seasonal variation in the ERA-Interim biases against A3 and A5, but the ERA5 bias changes from small positive values during the extended summer season to small negative values during winter (Table 5). This somewhat counterintuitive finding is a result of generally negative ERA5 biases for temperatures between −15°C and −25°C (see Figure 3b), which are typical of the winter period. The largest temperature biases are seen for buoy A4 in the coastal region, where ERA5 performs slightly worse than ERA-Interim, as measured by both bias and RMSE. However, as discussed in Section 4 below, it is possible that the use of a simple bilinear interpolation scheme may be increasing the calculated biases for buoy locations close to the coast.

Humidity variables from the reanalyses are compared with buoy measurements in Table 6 and Figure 4. Relative humidity with respect to ice in the reanalysis, calculated from reanalysis mixing ratio (ERA-Interim) or dew point (ERA5), temperature and pressure, appears to compare rather poorly with buoy measurements. However, unheated humidity sensors, such as those used on the buoys, are unable to measure supersaturation with respect to ice (Genthon et al., 2017) and a scatter plot of reanalysis against buoy relative humidity (Figure 4a) shows that, for much of the time, relative humidity is close to ice saturation in both the measurements and reanalysis. Around 85% of the buoy measurements indicate a relative humidity between 90% and 100%. The poor agreement for relative humidity may thus partly result from limitations in the measurements and from the small range of variation in this variable. With such a small variation in relative humidity, variations in humidity mixing ratio are largely controlled by variations in temperature, hence the performance of the reanalysis for this variable (Table 6 and Figure 4b) is similar to that for temperature.

Table 6

Validation Statistics for Reanalysis Humidity Interpolated to Buoy Locations

Buoy	Reanalysis	ERA mean	Buoy mean	Bias	RMSE	r
A3	ERA-Int.	1.72/92.1	1.65/95.9	0.07/−3.7*	0.25/6.68	0.979/0.639
A3	ERA5	1.61/92.1	1.64/95.9	−0.03/−3.7**	0.29/6.73	0.965/0.70
A4	ERA-Int.	1.50/95.7	1.41/95.6	0.09*/0.1	0.31/7.36	0.959/0.528
A4	ERA5	1.47/90.6	1.41/95.6	0.05/−5.0**	0.30/9.08	0.967/0.505
A5	ERA-Int.	1.26/95.2	1.25/97.4	0.01/−2.2*	0.25/5.35	0.959/0.639
A5	ERA5	1.19/94.0	1.25/97.4	−0.06/−3.4**	0.25/6.11	0.915/0.666

Note. Values are shown for mixing ratio (units: g kg^{-1})/relative humidity with respect to ice (units: %). Columns are as for Table 3. An asterisk indicates that the bias is statistically significant at the 5% level or better, a double asterisk at 1% or better.
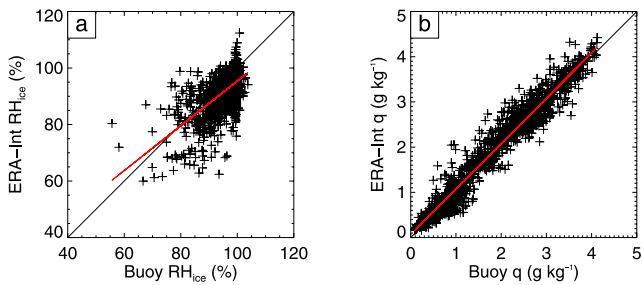
Figure 4. Six-hourly values of ERA-Interim relative humidity with respect to ice (a) and water vapor mixing ratio (b) plotted against corresponding measurements from buoy A3. The red lines are least squares regression fits to the data and the black lines indicate perfect agreement.

3.3. Wind

Table 7 shows validation statistics for reanalysis 10 m wind speed compared with a 10 m wind speed extrapolated from buoy measurements as described in Section 2.3. Both reanalyses show a consistent positive bias but examination of scatter plots of reanalysis wind speed against buoy wind speed (Figure 5) indicates that much of this bias comes from times when the buoy wind speed was less than around 3 m s^{-1}. While the quality control procedures described in Section 2.1 will have eliminated buoy data that were most badly affected by icing there are likely to be some occasions where icing reduced the measured wind speed but was not severe enough to be picked up by our quality control procedures. Restricting the validation to the months when our quality control procedure detects icing least frequently (January, February, and October–December) results in a small reduction in mean bias and RMSE but no change in correlation coefficients. At wind speeds greater than 5 m s^{-1} any ice will be rapidly removed from the wind monitor. If the comparison is restricted to these higher wind speeds the reanalysis biases all reduce to less than 0.2 m s^{-1} and are no longer statistically significant.

Tables 8 and 9 show validation statistics for the u- (zonal) and v- (meridional) components, respectively, of the 10 m wind against measurements from buoys A4 and A5, with the corresponding scatter plots for A5 shown in Figure 6. The wind components are simulated well in both reanalyses, with small (and not statistically significant) biases, from which it can be inferred that the reanalyses provide a good simulation of wind direction as well as wind speed. There is little difference in performance between ERA-Interim and ERA5.

3.4. Radiation

Tables 10 and 11 show validation statistics for daily mean downwelling shortwave and longwave radiation, respectively. Both reanalyses exhibit positive biases in downwelling shortwave radiation and corresponding negative biases in downwelling longwave radiation at all three buoy locations, with little difference in bias between the two reanalyses. However, the magnitude of the biases varies greatly between the buoy locations. While the reanalysis means at A3 and A4 are similar, biases at A3 are 2–3 times those seen at A4, located in coastal fast ice. Shortwave biases at A5 appear to be much smaller than those seen at A4 but the two records are not directly comparable as the record from A5 ends in early November while that from A4 continues to late February and thus includes the whole of the 2016–2017 summer season when shortwave radiation is at its highest. Correlation coefficients for shortwave radiation all exceed 0.9 and those for longwave radiation are only slightly lower, indicating that both reanalyses provide a good simulation of the variation of the radiation components on timescales from daily to seasonal.

Although the biases shown in Tables 10 and 11 are large and statistically significant, they need to be considered in the context of the accuracy of the measurements. Measurement uncertainties due to calibration uncertainties are around 5% of the sensor reading for the shortwave sensor and around 10% for the longwave sensor (Table 1). The biases for shortwave radiation (Table 10) lie outside these uncertainty limits while the longwave biases (Table 11) are comparable to the measurement uncertainty. In addition to calibration uncertainties, accumulation of snow and ice on the sensors during deployment will introduce additional measurement uncertainty. Icing of the shortwave sensor will reduce the radiation received by that sensor and could be contributing to the positive bias seen in the reanalyses while icing of the longwave sensor will generally result in an increase in the measured radiation, leading to an apparent negative bias in the reanalyses. Tables 10 and 11 also show validation statistics for the reanalyses against measurements from Halley Research Station (75.61°S, 26.27°W, see Figure 1), where radiation measurements were made using instruments with forced ventilation that
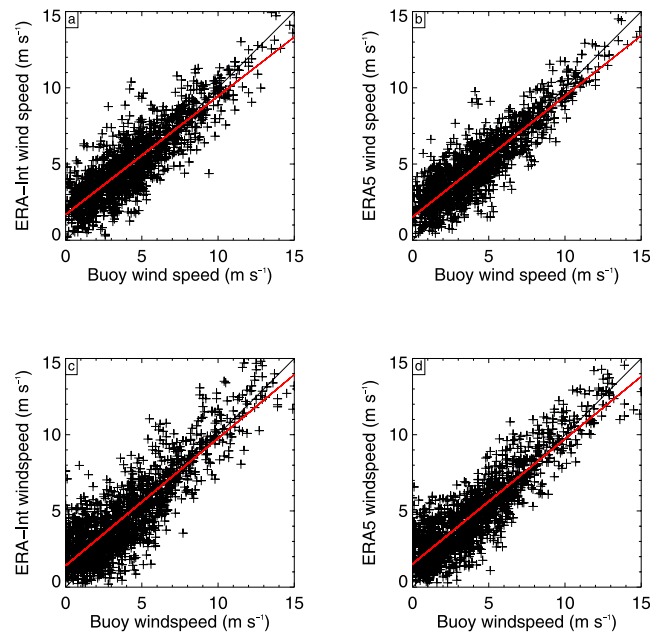
Table 7

Validation Statistics for Reanalysis 10 m Wind Speed Interpolated to Buoy Locations (Units: m s^{-1})

Buoy	Reanalysis	ERA mean	Buoy mean	Bias	RMSE	r
A3	ERA-Int.	5.05	4.33	0.71*	1.60	0.862
A3	ERA5	4.96	4.33	0.63*	1.44	0.889
A4	ERA-Int.	4.80	4.06	0.74*	1.79	0.835
A4	ERA5	4.85	4.06	0.79*	1.64	0.888
A5	ERA-Int.	5.65	4.88	0.76*	1.88	0.814
A5	ERA5	5.56	4.88	0.67*	1.67	0.856

Note. Buoy wind speeds have been extrapolated to the 10 m level as described in Section 2.3. Columns are as for Table 3. An asterisk indicates that the bias is statistically significant at the 5% level or better.

Figure 5. Six-hourly values of reanalysis 10 m wind speed, plotted against measurements from buoy A3 (panels (a) and (b)) and buoy A4 (panels (c) and (d)). The red lines are least squares regression fits to the data and the black lines indicate perfect agreement.

prevents icing of the sensors. Both reanalyses show much smaller biases relative to these measurements, which suggests that the biases seen relative to the buoy measurements may largely result from measurement errors due to snow and ice accumulation on the radiometers.

4. Discussion

We have carried out a comprehensive validation of the representation of near-surface meteorological variables over the Weddell Sea in the ERA-Interim and ERA5 reanalyses against measurements from three drifting buoys. Mean sea level pressure measurements from the buoys are reproduced with high accuracy by both reanalyses, suggesting that both products are capable of providing a good representation of the pressure field across the Weddell Sea and its variability on synoptic to seasonal timescales. This provides a sound foundation for the simulation of other aspects of surface meteorology.

The variability in near-surface air temperature measurements from the buoys is captured well in the ERA-Interim reanalysis (correlation coefficients >0.95) but this reanalysis has a mean warm bias of 1–2°C at the buoy locations which is mainly caused by very large warm biases at the lowest temperatures (5–10°C at −40°C, see Figure 3). The magnitudes and temperature dependence of the biases found in this study, are similar to those found in the western Weddell Sea by Jonassen et al. (2019) and to ERA-Interim temperature biases over Arctic sea ice (Wang et al., 2019). A possible cause of these warm biases is the use of a constant sea ice thickness of 1.5 m and the lack of any representation of snow cover on sea ice in the reanalysis model. Arduini et al. (2022) demonstrated that including a representation of snow cover in the ECMWF IFS model significantly improved surface temperature biases and the representation of rapid cooling events in 5-day forecasts over Arctic sea ice. The sea ice at the deployment sites of buoys A3 and A4 was significantly thicker than 1.5 m and was covered in 0.2–0.3 m of snow (Table 2). It is also likely that the ice thickness at these locations increased through the winter. The ERA-Interim reanalysis records accumulated snowfall of 266 and 183 mm water equivalent at A3 and A5, respectively, over the lifetime of the buoys,

Table 8
Validation Statistics for the Reanalysis u- (Zonal) Component of the 10 m Wind Interpolated to Buoy Locations

Buoy	Reanalysis	ERA mean	Buoy mean	Bias	RMSE	r
A4	ERA-Int.	−1.42	−1.46	0.04	1.75	0.916
A4	ERA5	−1.69	−1.46	−0.23	1.53	0.933
A5	ERA-Int.	1.36	1.09	0.27	1.62	0.932
A5	ERA5	1.33	1.09	0.25	1.41	0.949

Note. Buoy winds have been extrapolated to the 10 m level as described in Section 2.3. Columns are as for Table 3.

Table 9
Validation Statistics for the Reanalysis v- (Meridional) Component of the 10 m Wind Interpolated to Buoy Locations

Buoy	Reanalysis	ERA mean	Buoy mean	Bias	RMSE	r
A4	ERA-Int.	−0.28	−0.17	−0.11	1.61	0.883
A4	ERA5	−0.17	−0.17	−0.01	1.62	0.880
A5	ERA-Int.	1.48	1.21	0.26	1.65	0.908
A5	ERA5	1.38	1.21	0.16	1.47	0.924

Note. Buoy winds have been extrapolated to the 10 m level as described in Section 2.3. Columns are as for Table 3.

suggesting that the snow depth at these stations may have increased through the winter. However, measurements from the Snow Buoys adjacent to A3 and A5 indicate little change in snow depth over this period. The thinner ice and lack of a highly insulating snow cover in the reanalysis will lead to a larger conductive flux of heat through the ice to the atmosphere which could explain the warm biases seen in the reanalysis. The ice thickness at the deployment site of A5 was comparable to the 1.5 m used in the reanalysis and it is notable that the ERA-Interim warm bias is smallest at A5. The large warm biases seen at very low temperatures may also reflect the challenges of modeling the very stable boundary layer and sharp surface inversion that form under such conditions.

In contrast to the Arctic study of Wang et al. (2019), who found larger warm biases in ERA5 than in ERA-Interim, the warm biases at A3 and A5 in ERA5 are considerably smaller than those in ERA-Interim and are not statistically significant. Both reanalyses use the same simple representation of sea ice—1.5 m constant ice thickness and no snow cover—so, while this improvement could be due to small differences between the OSTIA and OSI SAF sea ice concentration products, it is more likely due to improved vertical resolution in the ERA5 atmospheric model and, possibly, improved model physics leading to a better representation of surface inversions under stable conditions. Temperature biases for buoy A4, which remained close to the coast throughout its lifetime, are much larger than those for A3 and A5 and, in contrast to A3 and A5, the ERA5 bias exceeds that for ERA-Interim. The ice and snow thicknesses measured at the time of the A4 deployment (3.3 and 0.32 m, respectively) were significantly larger than those measured at A3 and A5 (see Table 2) so reanalysis errors resulting from using a fixed 1.5 m ice thickness with no snow cover will be greatest at this location. It is not immediately clear, however, why ERA5 biases should exceed those for ERA-Interim at A4. The sea ice in the coastal region occupied by this buoy is spatially complex, with coastal polynyas opening and closing in response to changing weather conditions (Markus et al., 1998). These small-scale features will not be well-resolved in either the OSTIA or OSI SAF sea ice concentration products but are more likely to be represented in the higher-resolution ERA5. We know from the behavior of A4 that it remained in coastal fast ice for much of the winter but ERA temperatures interpolated to the buoy location may be influenced by
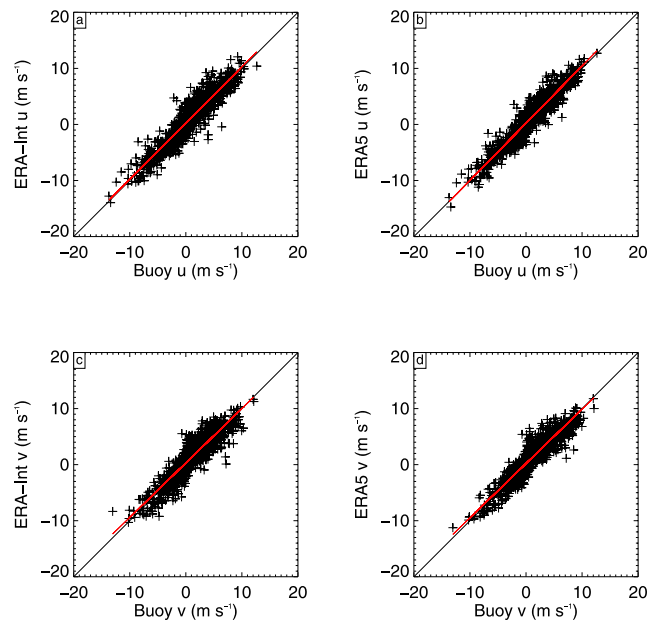

Figure 6. Six-hourly values of the zonal (*u*: a and b) and meridional (*v*: c and d) components of the 10 m wind from the reanalyses against extrapolated measurements from buoy A5. The red lines are least squares regression fits to the data and the black lines indicate perfect agreement.

Table 10

Validation Statistics for Daily Mean Downwelling Shortwave Radiation at the Buoy Locations and at Halley Station

Buoy	Reanalysis	ERA mean	Buoy mean	Bias	RMSE	r
A3	ERA-Int.	119.2	97.2	22.0*	58.8	0.907
A3	ERA5	120.8	97.2	23.6*	53.8	0.918
A4	ERA-Int.	110.5	98.5	12.0	42.4	0.951
A4	ERA5	108.8	98.5	10.3*	33.2	0.966
A5	ERA-Int.	56.9	51.8	5.1	30.1	0.921
A5	ERA5	57.5	51.8	5.7	27.4	0.923
Halley	ERA-Int	116.9	115.4	1.5	31.2	0.975
Halley	ERA5	120.7	115.4	5.3	23.6	0.986

Note. Halley statistics are for the calendar year of 2016. Columns are as for Table 3. An asterisk indicates that the bias is statistically significant at the 5% level or better.

warmer temperatures over nearby open water, particularly in ERA5, which is more likely to resolve small areas of open water. Another contributor to differences between the two reanalyses in the coastal region may be the higher-resolution land-sea mask used in the ERA5 product. At the location of A4 when it was stationary in fast ice, all of the grid points used to interpolate reanalysis temperatures to the buoy location were sea points in ERA5 but at least one in ERA-Interim was a land or coastal point. Land–sea temperature contrasts in this coastal region are high (King et al., 2021) and inclusion of colder land data in the calculation of the ERA-Interim interpolated temperature may have reduced the apparent temperature bias in this reanalysis.

Comparison of near-surface winds from the reanalyses with the buoy measurements suggests that both reanalyses provide a good representation of the mean wind and its variability. Mean biases are small and are probably within the uncertainty bounds of the measurements and those associated with extrapolating the buoy measurements to the 10 m level for comparison with the reanalyses. Reanalysis performance has improved slightly between ERA-Interim and ERA5, with the latter product exhibiting slightly smaller mean biases and RMSEs, and slightly larger correlation coefficients. As both reanalyses represent mslp to similar accuracy, the small improvement in the performance of ERA5 is probably a result of the higher resolution (both horizontal and vertical) and improved representation of boundary layer processes in this product.

Variability in daily means of observed downwelling short- and longwave radiation is reproduced quite well in both reanalyses, with correlation coefficients of the order of 0.9 but we find significant positive biases in shortwave radiation and corresponding negative biases in longwave radiation of similar magnitudes in both reanalyses. We cannot be certain whether these biases are genuine or if they result from measurement errors caused by the accumulation of snow and ice on the buoy radiometers. The observation that both reanalyses exhibit small biases against radiation measurements at Halley station (where the radiometers are kept clear of snow and ice) and the insignificant biases found against measurements from well-maintained radiometers at Ice Station Weddell (Jonassen et al., 2019) both support the latter viewpoint.

Our comparison of reanalysis data and buoy measurements suggests that both ERA-Interim and ERA5 are suitable for forcing ice-ocean models over Weddell Sea pack ice throughout the year. In particular, both reanalyses reproduce day-to-day variability in mslp, near-surface temperature and winds, and surface radiative fluxes remarkably well. Both reanalyses exhibit a significant warm bias in near-surface air temperature, which increases with decreasing temperature, but the mean bias for the two buoys deployed in drifting pack ice is much smaller in ERA5 than in ERA-Interim. These biases could be reduced in future reanalysis products by using a more sophisticated representation of sea ice that allowed for a variable ice thickness and included some representation of the insulating snow layer on top of the ice.

Table 11

Validation Statistics for Daily Mean Downwelling Longwave Radiation at the Buoy Locations and at Halley Station

Buoy	Reanalysis	ERA mean	Buoy mean	Bias	RMSE	r
A3	ERA-Int.	224.4	244.8	−20.4*	33.0	0.866
A3	ERA5	224.3	244.8	−20.5*	32.4	0.867
A4	ERA-Int.	221.7	229.3	−7.7*	21.8	0.864
A4	ERA5	221.5	229.3	−7.8*	21.8	0.861
A5	ERA-Int.	213.4	232.1	−18.7*	29.3	0.879
A5	ERA5	217.2	232.1	−14.4*	26.2	0.865
Halley	ERA-Int	202.9	205.4	−2.5	17.9	0.991
Halley	ERA5	200.3	205.4	−5.1	17.9	0.921

Note. Halley statistics are for the calendar year of 2016. Columns are as for Table 3. An asterisk indicates that the bias is statistically significant at the 5% level or better.

Our evaluation of the reanalyses has been limited to some extent by the quality of data available from the buoys. In particular, both wind and radiation measurements may be affected by icing of the sensors to a degree that is difficult to quantify. Further efforts are required to develop sensors and platforms that are less prone to icing or can detect when it is a problem. Measurements such as those reported here are needed for other regions of the Antarctic sea ice zone in order to study geographic variations in reanalysis performance. In the meantime, our assessment of the reanalyses provides a starting point for understanding the impact of uncertainties in the current generation of reanalyses on ice-ocean model simulations.

Data Availability Statement

Measurements from buoys A3, A4, and A5 from 15 January 2016 to 01 March 2017 were obtained from https://data.seaiceportal.de/gallery/index_new.php?lang=en_US%26active-tab1=method%26active-tab2=buoy (Grant: REKLIM-2013-04). Snow Buoy measurements are stored in PANGAEA (Nicolaus et al., 2021, https://doi.pangaea.de/10.1594/PANGAEA.875638). ERA-Interim and ERA5 data are available from the Copernicus Climate Data Store, https://cds.climate.copernicus.eu.

References

Anderson, P. S. (1994). A method for rescaling humidity sensors at temperatures well below freezing. *Journal of Atmospheric and Oceanic Technology*, *11*(5), 1388–1391. https://doi.org/10.1175/1520-0426(1994)011<1388:AMFRHS>2.0.CO;2

Andreas, E. L., Jordan, R. E., & Makshtas, A. P. (2005). Parameterizing turbulent exchange over sea ice: The Ice Station Weddell results. *Boundary-Layer Meteorology*, *114*(2), 439–460. https://doi.org/10.1007/s10546-004-1414-7

Arduini, G., Keeley, S., Day, J., Sandu, I., Zampieri, L., & Balsamo, G. (2022). On the importance of representing snow over sea-ice for simulating the Arctic boundary layer. *Journal of Advances in Modeling Earth Systems,* 14*(7*). https://doi.org/10.1029/2021MS002777

Dee, D. P., Uppala, S. M., Simmons, A. J., Berrisford, P., Poli, P., Kobayashi, S., et al. (2011). The ERA-Interim reanalysis: Configuration and performance of the data assimilation system. *Quarterly Journal of the Royal Meteorological Society*, *137*(656), 553–597. https://doi.org/10.1002/qj.828

Donlon, C. J., Martin, M., Stark, J., Roberts-Jones, J., Fiedler, E., & Wimmer, W. (2012). The operational sea surface temperature and sea ice analysis (OSTIA) system. *Remote Sensing of Environment,* 1*16*, 140–158. https://doi.org/10.1016/j.rse.2010.10.017

Genthon, C., Piard, L., Vignon, E., Madeleine, J. B., Casado, M., & Gallée, H. (2017). Atmospheric moisture supersaturation in the near-surface atmosphere at Dome C, Antarctic plateau. *Atmospheric Chemistry and Physics*, *17*(1), 691–704. https://doi.org/10.5194/acp-17-691-2017

Hersbach, H., Bell, B., Berrisford, P., Hirahara, S., Horányi, A., Muñoz-Sabater, J., et al. (2020). The ERA5 global reanalysis. *Quarterly Journal of the Royal Meteorological Society*, *146*(730), 1999–2049. https://doi.org/10.1002/qj.3803

Jackson, K., Wilkinson, J., Maksym, T., Meldrum, D., Beckers, J., Haas, C., & Mackenzie, D. (2013). A novel and low-cost sea ice mass balance buoy. *Journal of Atmospheric and Oceanic Technology*, *30*(11), 2676–2688. https://doi.org/10.1175/jtech-d-13-00058.1

Jonassen, M. O., Välisuo, I., Vihma, T., Uotila, P., Makshtas, A. P., & Launiainen, J. (2019). Assessment of atmospheric reanalyses with independent observations in the Weddell Sea, the Antarctic. *Journal of Geophysical Research: Atmospheres*, *124*(23), 12468–12484. https://doi.org/10.1029/2019JD030897

King, J. C. (2003). Validation of ECMWF sea level pressure analyses over the Bellingshausen sea, Antarctica. *Weather and Forecasting*, *18*(3), 536–540. https://doi.org/10.1175/1520-0434(2003)18<536:VOESLP>2.0.CO;2

King, J. C., Turner, J., Colwell, S., Lu, H., Orr, A., Phillips, T., et al. (2021). Inhomogeneity of the surface air temperature record from Halley, Antarctica. *Journal of Climate*, *34*(12), 4771–4783. https://doi.org/10.1175/jcli-d-20-0748.1

Lavergne, T., Sørensen, A. M., Kern, S., Tonboe, R., Notz, D., Aaboe, S., et al. (2019). Version 2 of the EUMETSAT OSI SAF and ESA CCI sea-ice concentration climate data records. *The Cryosphere*, *13*(1), 49–78. https://doi.org/10.5194/tc-13-49-2019

Markus, T., Kottmeier, C., & Fahrbach, E. (1998). Ice formation in coastal polynyas in the Weddell sea and their impact on oceanic salinity. In M. O. Jeffries (Ed.), *Antarctic sea ice: Physical processes, interactions and variability* (pp. 273–292). American Geophysical Union. https://doi.org/10.1029/AR074p0273

Neme, J., England, M. H., & Hogg, A. M. (2021). Seasonal and interannual variability of the Weddell gyre from a high-resolution global ocean-sea ice simulation during 1958–2018. *Journal of Geophysical Research: Oceans*, *126*(11), e2021JC017662. https://doi.org/10.1029/2021JC017662

Nicolaus, M., Hoppmann, M., Arndt, S., Hendricks, S., Katlein, C., Nicolaus, A., et al. (2021). Snow depth and air temperature seasonality on sea ice derived from snow buoy measurements. *Frontiers in Marine Science*, *8*. https://doi.org/10.3389/fmars.2021.655446

Stössel, A., Zhang, Z., & Vihma, T. (2011). The effect of alternative real-time wind forcing on Southern ocean sea ice simulations. *Journal of Geophysical Research*, *116*(C11), C11021. https://doi.org/10.1029/2011JC007328

Timmermann, R., Beckmann, A., & Hellmer, H. H. (2002). Simulations of ice-ocean dynamics in the Weddell sea 1. Model configuration and validation. *Journal of Geophysical Research: Oceans*, 107*(C*3), 10-1–10.11. https://doi.org/10.1029/2000JC000741

Vihma, T., Uotila, J., Cheng, B., & Launiainen, J. (2002). Surface heat budget over the Weddell sea: Buoy results and model comparisons. *Journal of Geophysical Research*, *107*(C2). https://doi.org/10.1029/2000JC000372

Wamser, C., & Martinson, D. G. (1993). Drag coefficients for winter Antarctic pack ice. *Journal of Geophysical Research: Oceans*, *98*(C7), 12431–12437. https://doi.org/10.1029/93JC00655

Wang, C., Graham, R. M., Wang, K., Gerland, S., & Granskog, M. A. (2019). Comparison of ERA5 and ERA-Interim near-surface air temperature, snowfall and precipitation over Arctic sea ice: Effects on sea ice thermodynamics and evolution. *The Cryosphere*, *13*(6), 1661–1679. https://doi.org/10.5194/tc-13-1661-2019

Weiss, A. I., King, J., Lachlan-Cope, T., & Ladkin, R. (2011). On the effective aerodynamic and scalar roughness length of Weddell sea ice. *Journal of Geophysical Research*, *116*(D19), D19119. https://doi.org/10.1029/2011JD015949